Electroactive molecularly imprinted nano-polymers (nanoMIPs)-based nanocomposite platform for the selective electrochemical detection of amphetamine

Florina Truta[1], Alvaro Garcia Cruz[2], Mihaela Tertis[1], Christopher Zaleski[2], Gyako Adamu[2], Natalie S. Allcock,[3] Maria Suciu[4,5], Maria-Georgia Ștefan[6], Béla Kiss[6], Elena Piletska[2], Karolien De Wael[7,8], Sergey A. Piletsky[2], Cecilia Cristea[1,*]

[1] Department of Analytical Chemistry, "Iuliu Hatieganu" University of Medicine and Pharmacy, 4 Louis Pasteur Street, 400349 Cluj-Napoca, Romania

[2] Chemistry Department, College of Science and Engineering, University of Leicester, University Rd, Leicester LE1 7RH, United Kingdom

[3] University of Leicester Core Biotechnology Services Electron Microscopy Facility, LE1 7RH, UK

[4] Electron Microscopy Centre "C. Craciun", Biology and Geology Faculty, Babes-Bolyai University Cluj-Napoca, 5-7 Clinicilor Str. 400006 Cluj-Napoca, Romania

[5] National Institute for Research and Development of Isotopic and Molecular Technologies, 67-103 Donath Street 400293 Cluj-Napoca, Romania

[6] Department of Toxicology, Faculty of Pharmacy, Iuliu Hatieganu University of Medicine, and Pharmacy, 6A Louis Pasteur Street, 400349 Cluj-Napoca, Romania

[7] University of Antwerp, A Sense Lab, Groenenborgerlaan 171, B-2020 Antwerp, Belgium

[8] University of Antwerp, NANOlab Ctr Excellence, Groenenborgerlaan 171, B-2010 Antwerp, Belgium

***Correspondence**

Cecilia Cristea

ccristea@umfcluj.ro

ABSTRACT

A highly sensitive and portable electrochemical sensor based on electroactive molecularly imprinted nanopolymers (nanoMIPs) was developed.

NanoMIPs were computationally designed for specific recognition of amphetamine, and then synthetized using solid phase synthesis. NanoMIPs were immobilized on screen-printed carbon electrodes using a composite film comprising chitosan, nanoMIPs, and graphene oxide, the combination ratio between these nanocomponents being established after optimization.

Ferrocenylmethyl methacrylate was incorporated in nanoMIPs and the presence of the ferrocene function allowed electrochemical detection, the signal recorded for the electrochemical oxidation of ferrocene proving to be dependent on the presence of amphetamine in the nanMIPs cavities. The sensor was tested successfully on street samples, with high sensitivity and satisfactory recoveries (from 100.9% to 107.6%). These results were validated with UPL-MS/MS. The present technology could be potentially used in forensics and to help the selective determination of amphetamine in street samples containing this drug of abuse.

Keywords: nanoMIPs; amphetamine; electrochemical sensors; illicit drug detection.

Graphical abstract: portable sensor device using nanoMIPs-based nanocomposite platform for the selective amphetamine electrochemical detection

1. Introduction

Illicit drugs consumption remains a public threat worldwide and represents a significant challenge for the local authorities [1]. Of these, amphetamine (AMF) is a central nervous system stimulant but in the same time a FDA approved treatment of narcolepsy and ADHD [2,3]. The acute administration of AMF could lead to several desirable effects such as euphoria, physical fearlessness, increased arousal or wakefulness, hyperactivity, and impulsivity [4]. Unfortunately, these effects have led to an abuse of AMF in our society [5]. AMF abuse provokes hyperthermia, tachycardia, palpitation, increased breathing rate, increased blood pressure, and in worst cases, even death [6].

AMF represents the second most used stimulant drug in Europe, with 1.4 million young adults (15-34 years) consumers reported only in the last few year (1.4% of this age group) [7]. In 2019, 34 000 seizures of AMF were reported by the EU Member States, amounting to 17 tons while in 2018 the reported amount was of about 8 tons, representing an important increase, with the quantity increasing over the last four years [8]. Hence, the law enforcement agencies (LEAs) requested new tools and devices for decentralized detection of illicit substances from street samples [9].

Usually, the authorities analyze the unknown street samples from harbors, airports, or clandestine laboratories using color tests or portable spectroscopic analysis. These tests are only presumptive and depending on the results the confiscated samples are sent to the laboratory for further tests [10]. In the laboratory the most common methods for drugs identification are capillary electrophoresis, near infrared spectroscopy, gas chromatography and liquid chromatography [11]. Unfortunately, these methods require strict laboratory conditions and trained personnel, and the length of the analysis prevents the authorities from acting immediately [12]. Some alternatives to these tests which could be used in the field are the portable spectroscopic methods (i.e. portable Raman and portable infrared spectroscopy). Even if these methods could be used in field, are fast and user-friendly, they require specialized personnel for data interpretation, while the cost per analysis is significant [13]. On the contrary, the electrochemical methods offer a fast, accurate, portable, and low-cost alternative for drugs identification. Electrochemical sensors are an alternative preferred for in field analysis due to their simplicity, portability, fast response, and also because they are easy to adopt and implement for the detection of illicit drugs [4,14].

The AMF can’t be directly detected using the electrochemical methods because it is not an electroactive compound. In this regard, an electroactive molecularly imprinted nanopolymer (nanoMIPs) for AMF detection was synthesized and applied in this study for the ultra-selective and sensitive detection of AMF.

MIPs are often referred to as synthetic antibodies due to their recognition mechanism [15]. NanoMIPs are produced by solid phase synthesis, in the presence of the template molecule (the

molecule that will be detected afterwards). After the extraction of nanoMIPs from the solid phase their structure acquire template complementary cavities (in terms of size, shape, and complementary binding sites), which can rebind the target molecule, even in the presence of interference compounds [16]. The principal advantage of the nanoMIPs based sensors are the robustness, specificity, high affinity and selectivity in biological and street samples and the lower price. The designing of nanoMIPs at nano dimensional scale demonstrated an enhancement in the surface-to-volume ratio thus making binding sites more accessible for the target analyte [14,17–19].

The current study takes advantage of the use of electroactive nanoMIPs-based composite for the selective capture of AMF from real and complex samples such as seized drug samples. The printed nanopolymer was synthesized in the presence of the AMF template, so that the cavities in the polymer formed after removing the template have the right size and affinity with the template molecule.

The sensor response relies on the nanoMIPs actuation as a result of the recognition of the analyte. This actuation mechanism is known as "Induced fit" in enzymes [20,21]. The analyte recognition triggers the nanoMIPs conformational changes. As a result, the ferrocene electroactive moieties are exposed, increasing the electron transfer rate. Therefore, the actuation is highly selective, and the analyte concentration is directly related to the change in the current response of the sensor. The nanoMIPs display the characteristic ferrocene electrochemical signal, which can be monitored as a redox marker during electrochemical determinations.

Therefore, the detection is based on the evaluation of the electrochemical signal of the nanoMIPs. Following the oxidation signal of ferrocene from nanoMIPs, it was found that it increases after the capture (rebinding) of AMF molecules, the increase being proportional to the concentration of AMF in the solution from which the rebinding was carried out over a large concentration range, thus proving a good control over the detection process. This technology was already reported on other analytes [14,22,23], and was adapted for the target analyte with the help of molecular modeling, the step that allowed the selection of the most compatible monomers, cross-linkers or stabilizers for the selective immobilization and detection of AMF. This detection strategy has been successfully applied for the selective detection of AMF on street samples.

2. Materials and methods

2.1. Materials and instrumentation

All reagents used in this study were of analytical grade and were used as received from the manufacturer without further purification. All solutions were prepared with ultrapure water (18.2 MΩ, Millipore Simplicity). Amphetamine (base HCl; solid) was purchased from Cayman Chemicals, while, polyethyleneimine (PEI), aniline, 2',2'-bitiophene, tetrabutylammonium

hexafluorophosphate (4-BAGFPR), chitosan, dipotassium phosphate (K_2HPO_4), potassium dihydrogen phosphate (KH_2PO_4), potassium chloride (KCl), hydrochloric acid (HCl), sulfuric acid (H_2SO_4), nitric acid (HNO_3), potassium ferrocyanide ($[Fe(CN)_6]^{4-}$), potassium ferricyanide ($[Fe(CN)_6]^{3-}$), sodium hydroxide (NaOH), were purchased from Merck. Graphene oxide (GPHOx) 4 mg mL^{-1} suspension in water was provided by Metrohm Dropsens (Oviedo, Spain). Phosphate buffer saline (PBS) solution of 0.1 M with 0.1 M KCl was used as the supporting electrolyte and it was prepared with K_2HPO_4 and KH_2PO_4, adjusted to the mentioned values of pH with either NaOH or HCl.

Amphetamine solution in methanol (Cerilliant, standard solution of 1 mg mL^{-1}), 3-aminopropyltrimethyloxysilane (APTES), N-(6-aminohexyl)aminomethyltriethoxysilane (AHAMTES), glutaraldehyde, 1,2-Bis(triethoxysilyl)ethane (BTSE), N-hydroxy-succinimide (NHS), Ferrocene methylmethacrylate (FcMMA), 2-Hydroxyethyl methacrylate (HEM), Itaconic acid (ITA), 1-ethyl-3-(3-dimethylaminopropyl)-carbodiimide hydrochloride (EDC), ethylene glycol dimethacrylate (EGDMA), trimethylolpropane trimethacrylate (TRIM), and pentaerythritol tetrakis(3-mercaptopropionate) (PETMP), and sodium hydroxide (NaOH), were from Sigma-Aldrich, UK. Phosphate buffered saline (PBS) consisted of phosphate buffer (0.1 M), potassium chloride (0.003 M), and sodium chloride (0.140 M), pH 7.4 was procured prom Gibco Life technologies Ltd, UK. Dimethylformamide (DMF), acetonitrile HPLC Grade and acetone were from Fisher Scientific, UK. The N,N-diethyldithiocarbamic acid benzyl ester was purchased from TCI Europe (Belgium) and used as initiator, transfer agent, and terminator.

The polymerization reaction was completed using UV sources (Philips HB / 171 / A, 0.5 W cm^{-1},4 x 15 W lamps). Afterwards the solid phase extraction cartridges (SPE) with polyethylene frit (20 µm porosity, Supelco) were used for the elution of nanoMIPs. A nitrogen plasma cleaner was used to activate electrode surface (Emitech, K1050X RF Plasma Cleaner, 50 W, 13.56 MHz RF for 5 minutes). All the electrochemical measurements were performed by using a Potentiostat/Galvanostat/Impedance Analyzer (PalmSens EmStat3Blue) equipped with a cable connector for screen-printed electrodes and the PSTrace software (PalmSens, Netherlands) and a potentiostat/galvanostat Autolab PGSTAT 302N (Metrohm, Utrecht, The Netherlands) equipped with the associated NOVA 1.10.4 software.

All the SPEs with a silver pseudo reference, a carbon counter electrode and with different working electrodes: graphite-based, such as or modified with GPH and MWCNTs were provided by Dropsens Metrohm (Spain and UK, respectively). The data analysis and the creation of figures were performed using the Origin8.5 software (OriginLab, USA). For a better visualization, all the DPV voltammograms presented here were baseline-corrected using the moving average filter included in the NOVA 1.10.4 software (window size 1), without affecting the results. No other manipulation of the results was performed apart from this baseline correction provide the NOVA 1.10.4 software which was performed only for a better visual comparison of the voltammograms.

2.2. NanoMIP molecular modelling

Computational modelling of nanoMIP is based on the screening and selection of functional monomers using molecular mechanics [24,25] . The software package used was Sybyl ™ version 7.3 (Tripos Inc.) in a Gnome 2.28.2 desktop environment (CentOS Linux 7 operating system) and carried out in an HP Elite-Desk with two Intel Core ™Duo CPU E8400 and 3GHz processors.

All the details related to the modelling are presented in the ***Supplementary Information S1 1.1..***

2.3. NanoMIP synthesis

The synthesis of nanoMIPs was performed using the solid phase synthesis, and all the details are presented in the ***Supplementary Information S1 1.2***..

2.4. Sensors elaboration

nanoMIP suspension embedded in chitosan

A suspension of nanoMIPs in chitosan was used for the immobilization of the nanostructures at the electrode' s surface. Thus, 0.4 g of chitosan were dissolved in 15 mL of 0.5 M HCl. Subsequently, the solution was ultrasonicated for 1 h, then stirred for 2 h using a magnetic stirrer. The obtained solution was filtered and stored at 4^{o}C until use. Afterward, the chitosan solution was combined with nanoMIPs suspension (0.1 mg mL^{-1}) in different ratios, and the obtained suspension was drop-casted onto the surfaces of the SPEs using low retention tips and small volumes (2.5 μL) of suspension, which was previously well homogenized with the help of a mixer. The electrodes were dried in the oven for 30 minutes and then incubated with different concentrations of AMF solution. After the incubation, the electrodes were tested with a PBS pH 7.4 solution via DPV.

nanoMIP suspension embedded in chitosan and GPHOx

A suspension of nanoMIPs (0.1 mg mL^{-1}) in chitosan (0.5 mg mL^{-1}) and GPHOx (1 mg mL^{-1}) was also used for the immobilization of functionalization nanoparticles onto the electrode. The chitosan solution was prepared as in the previews case, and afterwards was combined with nanoMIPs suspension in 1 to 2 ratio. Simultaneously, a stock solution of GPHOx with a concentration of 4 mg mL^{-1} was ultrasonicated for 15 minutes and was added in the suspension mentioned above to obtain a 1 mg mL^{-1} final concentration. Afterward, the suspension was drop-casted onto the surfaces of the SPEs using low retention tips and small volumes (2.5 μL) of suspension, which was previously well homogenized with the help of a mixer. The obtained functionalized electrodes were dried in the oven for 30 minutes. After the drying step the electrodes were reduced using Cyclic Voltametry (CV) (potential range from 0.5 V to -1.4 V, scan rate 0.5 V s^{-1}, 10 cycles) in a solution containing PBS pH 7.4 to transform GPHOx into reduced GPHOx (rGPHOx), which has higher electrical conductivity than the oxidized form of graphene, and then incubated with different AMF solutions with different concentrations. After

the incubation, the electrodes were tested in PBS pH 7.4 solution via DPV to record the ferrocene signal from the nanoMIPs structure after the contact with the target analyte.
Other methods were also tried for the deposition of nanoMIPs onto the SPEs, such as: deposition of nanoMIPs ink embedded in PEI, PANI and bithiophene polymer layers. These approaches were not successful because the stability of the films was poor, and led to unsatisfactory analytical performance; therefore the results were not presented in this manuscript (see the ***Supplementary information S2 2.1.*** for more details).

2.5. Characterization of the nanoMIPs

For the characterization of the nanoMIPs, 1 mL of suspension was sonicated for 1 minute to disrupt potential agglomerates. For the nanopolymer characterization, Transmission Electron Microscopy (TEM) images were obtained using a JEOL JEM-1400 TEM equipped with a 120kV Tungsten Filament and an EMSIS Xarosa 10MP digital camera. The size of the nanoparticles was estimated using ImageJ v. 151o software. Nanopolymer colloids were sonicated for 2 minutes, and then 10 µL of sample were let to adsorb for 25 minutes to a carbon film grid (AGS160 - Agar Scientific Ltd). Carbon grids were previously glow discharged in a Quorum Gloqube for 15 s at 20 mA. The elemental analysis and SEM images were captured at an accelerating voltage of 10 kV using a field emission gun (FEG) and an Environmental Scanning Electron Microscope (ESEM) FEI Quanta 650 FEG SEM equipped with energy dispersive X-ray spectrometer (EDX) and Electron Backscatter Diffraction . For all the samples, the accelerating voltage used was 5 or 10 kV, respectively. The hydrodynamic diameter and polydispersity index were measured using a Dynamic Light Scattering (DLS) using a Zetasizer Nano (Nano-S) analyser from Malvern Instruments Ltd. (Malvern, UK). For these measurements, 1 mL solution of nanoparticles was previously sonicated for 1 min to disrupt potential agglomerates.

2.6. Electrochemical measurements

Electrochemical characterization of the sensors based on nanoMIPs, after each modification step, was performed by CV (potential rage from -0.5 V to 1 V, scan rate 0.1 V/s, 2 cycles), and by Electrochemical Impedance Spectroscopy (EIS) (61 frequencies from 0.1 to 100000 Hz; open circuit potential (OCP)) in the presence of 5 Mm $[Fe(CN)_6]^{4-/3-}$ in 0.1 M KCl.
Electrochemical response of sensors was investigated by using Differential Pulse Voltammetry (DPV) in the potential range from -0.4 to 0.4 V (vs Ag/AgCl), scan rate of 33 mV s^{-1}, modulation amplitude 200 mV, modulation time at 20 ms and step potential of 50 mV. Samples (100 µL) were analyzed by drop casting on the sensor surface and incubating for 30 minutes. Then, the DPV measurements were assessed in triplicates. After measuring the voltammetric sensor response, the difference between the current obtained at different drugs concentrations and the current obtained after the incubation with a solution without AMF was calculated ($I-I_0$). Thus, calibration plots were obtained by representing the value of the current variation against the AMF concentration. The limit of detection (LOD) was calculated conventionally form calibration curves using the following equation $LOD=[blank+(3.3\times STD_{blank})]/slope$, where the

blank is the measurement at zero concentration of the analyte and the STD is the standard deviation [26–28].

2.7. Seized illicit drug samples analyzed by UPLC-MS/MS

An ultra performance liquid chromatograph-tandem mass spectrometer (UPLC-MS/MS) was used to validate the sensor measurements and analyse the street samples. Thus, a calibration plot was prepared as follows: an AMF stock solution in acetonitrile (156 µg mL^{-1}, equivalent to 1.15 mM) was prepared, and then diluted to obtain standard solutions with concentrations ranging from 80 ng mL^{-1} to 1200 ng mL^{-1} (from 592 nM to 8875 nM). Samples and standards solutions were prepared using a mobile phase comprising 2.5 mM ammonium acetate + 0.1% formic acid in water (A) and acetonitrile (B), (85:15, A:B, v/v). All the details are presented in the ***Supplementary Information Section S1 1.3.***).

2.8. Seized drug samples assessment

Sensors specific for AMF were prepared by the protocol described in **Section 2.4**. These sensors were employed to analyse "street" samples and the results were validated with those obtained by a UPLC-MS procedure. The concentration of the solution obtained after dissolving the confiscated "street" samples was determined by using the standard addition method. The method prevents the influence of the matrix and different interfering substances [14]. In this method, a series of AMF standard solutions are spiked with the same amount of the real samples with unknown concentration. From these measurements, a calibration plot is obtained. After the linear regression, the extrapolation method is used to calculate the unknown concentration of AMF. Initially, AMF "street" samples were dissolved in methanol (1 mg mL^{-1}). These samples were then diluted (5,000-150,000 fold). For that, 100 µL sample were diluted (5,000-150,000 fold) in 5 mM PBS. Afterwards, 50 µL of sample were added to 50 µL of PBS pH 7.4, and then to 50 µL of each standard, following the known protocol for the standard addition method.
Electrochemical measurements were performed as follows: each sample was incubated for 30 minutes on the sensor, then the sensor response for each spiked standard was measured by using DPV. The calibration was obtained by plotting the sensor current response against AMF concentration. The DPV potential range applied was from -0.9 to +0.4 V; with a scan rate of 33 mV s^{-1}, equilibration time of 5 s, pulse potential at 200 mV and pulse time of 50 ms.

3. Results and Discussions

3.1. Synthesis and characterization of electroactive polymers

The synthesized nanoMIPs were characterized before being used for the sensor design, to establish their dimensions, shape and other relevant physical properties. The hydrodynamic diameter of the nanoMIPs was found at 269.6 ± 28 nm (**Figure 1 (B)**), which shows that in aqueous solution the nanoparticles are surrounded by a stable layer of water, typical for

hydrophilic polymers. STEM image (**Figure 1 (A)**) shows an aggregation of homogenous round particles with a smooth surface. The aggregation is most likely the result of drying and surface tension on the grid surface. TEM measurements for nanoMIPs shown discrete homogeneous spherical particles with a size at 82±9 nm as shown in **Figure 1 (C; a and b**. The polydispersity index (PDI) was found at 0.278, which is acceptable considering that for polymer-based nanoparticle the acceptable PDI values in practice are around 0.2 [29], indicating that the particles are homogenous distributed.

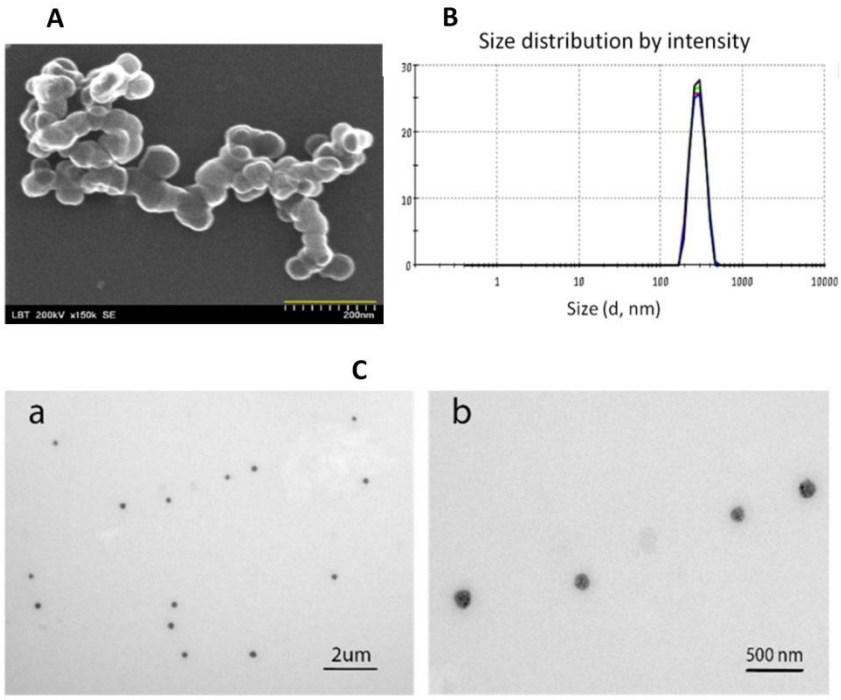

Figure 1. (A) STEM image for nanoMIP specific for amphetamine with a scale bar at 200 nm; (B) DLS measurement, Intensity signal against particle size; (C) TEM images for nanoMIP specific for amphetamine with a scale bar at (a) 2 µm and (b) 500 nm.

3.2. Electrochemical detection of amphetamine

3.2.1. Electrochemical characterization of the sensors based on nanoMIPs and chitosan

Different amounts of chitosan and nanoMIPs suspension were drop-casted onto the SPEs, and different combination ratios of these two components were tested to establish the optimal composition for the suspension. 10 µL of chitosan (2%) and nanoMIPs (0.1 mg mL^{-1}) suspensions prepared by using combination ratio of 1:1, and 1:2, respectively were deposited on the electrode. It was observed that the best results were obtained in the case of the 1:2 combination ratio between chitosan and nanoMIPs.

Another strategy was to modify the SPEs with 20 µL of a suspension containing 2% chitosan and nanoMIPs 0.1 mg mL^{-1} in combination ratio of 1:1 and 1:2, respectively, and the best results

were obtained again in the case of the 1:2 combination ratio. Comparing the results obtained after the deposition of 10 µL, and 20 µL of suspension, it was observed that the 10 µL deposition is more suitable, and the deposed film is more stable (does not peel off) and uniform (optimization data not presented).

The optimized nanoMIPs and rGPHOx based sensor step-by-step modification in GO/SPEs surface properties were evaluated by EIS and CV in the presence of a solution containing 5 mM $[Fe(CN)_6]^{4-/3-}$ prepared in 0.1 M KCl. The representation in the form of cyclic voltammograms of the CV data and Nyquist diagrams of the impedance data can be seen in **Figure 2(A)**, and **Figure 2(B)**, respectively.

The electrochemical properties of the surface of the sensor based on carbon SPE functionalized with chitosan, nanoMIPs and reduced GPHOx were evaluated using the redox probe $[Fe(CN)_6]^{3-/4-}$ and CV. Electrochemical characterization was also performed using EIS tests. The CV and EIS results obtained when testing the electrode surface after each stage of modification are further discussed and presented in **Figure 2(A)**. First, the cyclic voltammogram was plotted in the presence of 5 mM of $[Fe(CN)_6]^{3-/4-}$ for bare SPE based on carbon and the well-known aspect of the quasi-reversible voltammogram can be observed, with peak-to-peak separation of 218 mV and with the oxidation/reduction peak intensity of 153 µA/-143 µA. The modification of the surface with chitosan caused an increase in the current signal to 184 µA/-185 µA, simultaneously with a decrease in peak-to-peak separation of 128 mV. The properties of chitosan, namely its high surface area and outstanding electrical conductivity, are well known and have been widely employed for the modification of electrodes in sensors [30,31]. The subsequent modification of the surface with chitosan:GPHOx composite material determined a decrease of the signal intensity to 176 µA/-177 µA and an increase of the peak-to-peak separation to 146 mV, due to the presence of GPHOx, which has low electrical conductivity [32]. The use of GPHOx was necessary because graphene derivatives with higher conductivity are more difficult to solubilize in aqueous medium and it would be difficult to obtain a homogeneous and stable suspension in the chitosan solution. In practice, after modifying the electrodes with GPHOx, the surface undergoes an electrochemical reduction process [33], performed by CV. After the electrochemical reduction in 0.1 M PBS of pH 7.2, an important signal intensity increasing was observed, reaching 379 µA/-391 uA, with a peak-to-peak separation of 153 mV. The optimized configuration for the sensor, which also contains nanoMIPs for ANF, caused a decrease in the current signal to 181 µA/-197 uA, with a value of 105 mV for peak-to-peak separation. This behaviour is justified by the presence of nanoMIPs in the composite film deposited on the electrode surface, since the nanoMIPs have poor electrical conductivity. All these changes in the position and signal intensity of the redox probe are proofs of the successful modification of the electrode. The data obtained with the help of the CV were verified and confirmed by EIS. Thus, in **Figure 2(B)** you can see the Nyquist diagrams for the same electrode configurations. The most important parameter for comparing the surface conductivity is the charge transfer resistance (R_{ct}), which is represented in the diagram of the diameter of a semicircle. The smaller this diameter is, the higher of the electrical conductivity of the surface is. For the unmodified carbon

electrode, a value of R_{ct}=525 Ω was obtained, after functionalization with chitosan this decreased to 27 Ω. The addition of GPHOx in the composite film increased the R_{ct} to 35 Ω. The electrochemical reduction of GPHOx determines the increase of the conductivity of the film and an R_{ct} value of 8 Ω and the presence of nanoMIPs in the film increases the R_{ct} to 39 Ω.
Therefore, subsequent tests were performed using this configuration, obtained after the deposition of 10 µL chitosan: nanoMIPs 1:2 suspension. The results obtained after the deposition of different concentrations of AMF are presented in **Figure S3 (*Supplementary Information Section S2 2.2*)**

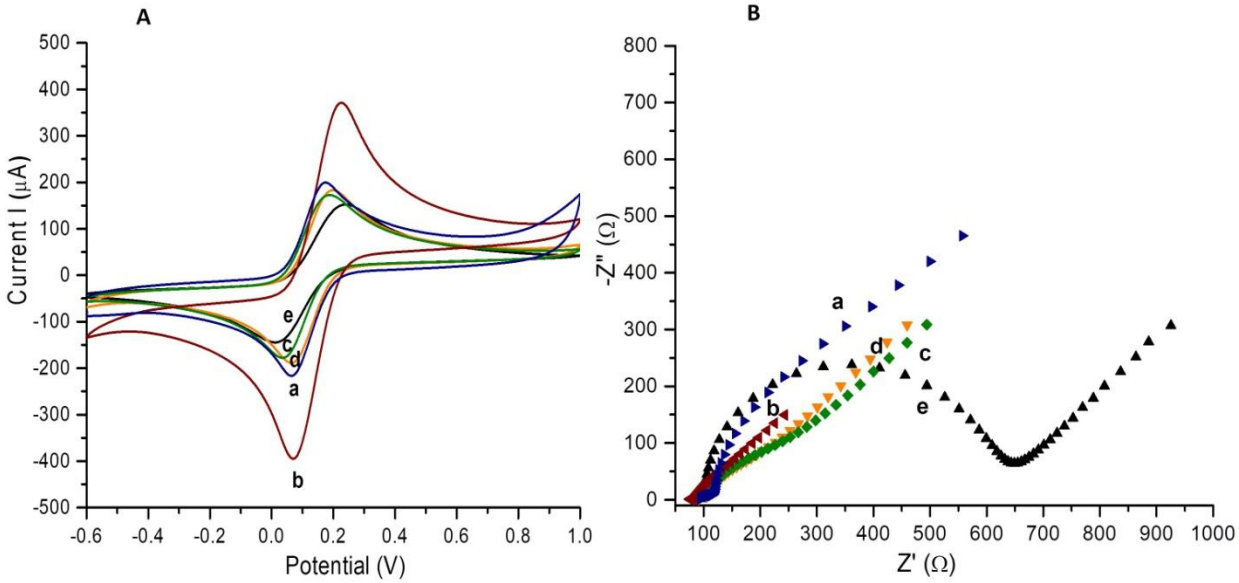

Figure 2. (**A**) Cyclic voltammograms and (**B**) Nyquist plots of EIS obtained in the presence of 5 mM $[Fe(CN)_6]^{3-/4-}$ in 0.1 M KCl for **(e) –** bare graphite-based SPE; **(d) –** SPE modified with chitosan; **(c)** –SPE modified with chitosan and GPHOx; **(b) –** SPE modified with reduced GPHOx and **(a) –** SPEs modified with nanoMIPs: Chitosan+GPHOx = 2:1 (optimized sensor).

3.2.2. Characterization and optimization of the sensors

The morphostructural characterization of the film deposited on the surface of the electrode, which contains nanoMIPs embedded in chitosan, respectively nanoMIPs and GPHOx embedded in chitosan, was performed using SEM. TEM investigation was also applied for the characterization of the suspension obtained in each case (**Figure S4)**. From the results presented in **Figure S4(A)** it is observed that in the absence of GPHOx, the film on the electrode shows cracks and unevenness. These problems disappeared after the introduction of GPHOx nanomaterial in the film. Also, in the presence of GPHOx it was observed that the distribution of nanoMIPs on the electrode surface is more uniform (**Figure S4(B)**). The TEM images obtained for the suspension with nanoMIPs, GPHOx and chitosan (**Figure S4(D)**) show a uniform

distribution of GPHOx sheets, which are important for improving the analytical performance of the sensor as mentioned in the literature [34]. The suspension of nanoMIPs in chitosan (**Figure S4(C)**) shows a uniform distribution of polymeric nanostructures in the chitosan solution, which is the premise of homogeneous and reproducible deposits.

3.3. Analytical performance of the nanoMIPs-based sensors

Amphetamine sensor based on nanoMIPs and chitosan

Increasing concentrations of AMF were incubated on the graphite SPEs modified with chitosan 0.5 mg mL^{-1} and a 0.1 mg mL^{-1} ethanolic suspension of nanoMIPs in a combination ratio of 1:2. It can be observed that AMF could be detected in a linear range from 1 nM to 250 nM (**Figure 3(A)**), with a detection limit (LOD) of 0.3 nM, a limit of quantification (LOQ) of 1 nM, a sensitivity of 0.82 μA nM^{-1} for the first concentration domain, and 0.04 μA nM^{-1} for the second one, and an average RSD of 2.97%. In the calibration curve presented in **Figure 3(B)**, the differences between current intensities at different concentrations and the current intensity obtained in the case of incubation with 25 μL of 0.1 M PBS pH 7.4 (0 nM AMF) were represented.

Amphetamine sensor based on nanoMIPs, GPHOx and chitosan

In the case of the sensor based on graphite SPEs modified with chitosan 0.5 mg mL^{-1}, GPHOx 1 mg mL^{-1} and nanoMIPs 0.1 mg mL^{-1} in a combination ratio of 1:2, the DPV tests performed in the presence of 100 μL of 0.1 M PBS of pH 7.4 after 30 minutes of preconcentration with AMF solutions of different concentrations, are presented in **Figure 3(C)**. It was observed that AMF could be detected in a linear range from 1 nM to 200 nM (**Figure 3(C)**), with a LOD of 0.3 nM, a LOQ of 1 nM, a sensitivity of 2.68 μA nM^{-1}, and an average RSD of 3.69%. In the calibration curve presented in **Figure 3(D),** the differences between current intensity at different concentrations and the current intensity obtained in the case of preconcentration with 25 μL of 0.1 M PBS of pH 7.4 (0 nM AMF) were represented.

It can be observed that after the addition of GPHOx to the composite film on the electrode along with nanoMIPs and chitosan, the sensitivity for AMF detection increased more than three times. A comparison between the results obtained after the incubation of AMF on the optimized platform, on the chitosan platform, and on the unmodified SPEs, respectively was performed to prove the usability of the nanoMIPs for AMF detection. Thus, SPEs were modified with 10 μL of chitosan 0.5 mg mL^{-1}, and was dried in the oven for 30 minutes. Afterwards, the modified electrode was incubated with different concentrations of AMF for 30 minutes, and then was tested in PBS pH 7.4 using DPV. Unmodified graphite SPEs were also incubated with the same concentrations of AMF and were tested in the same way. All these tests were performed in triplicates.

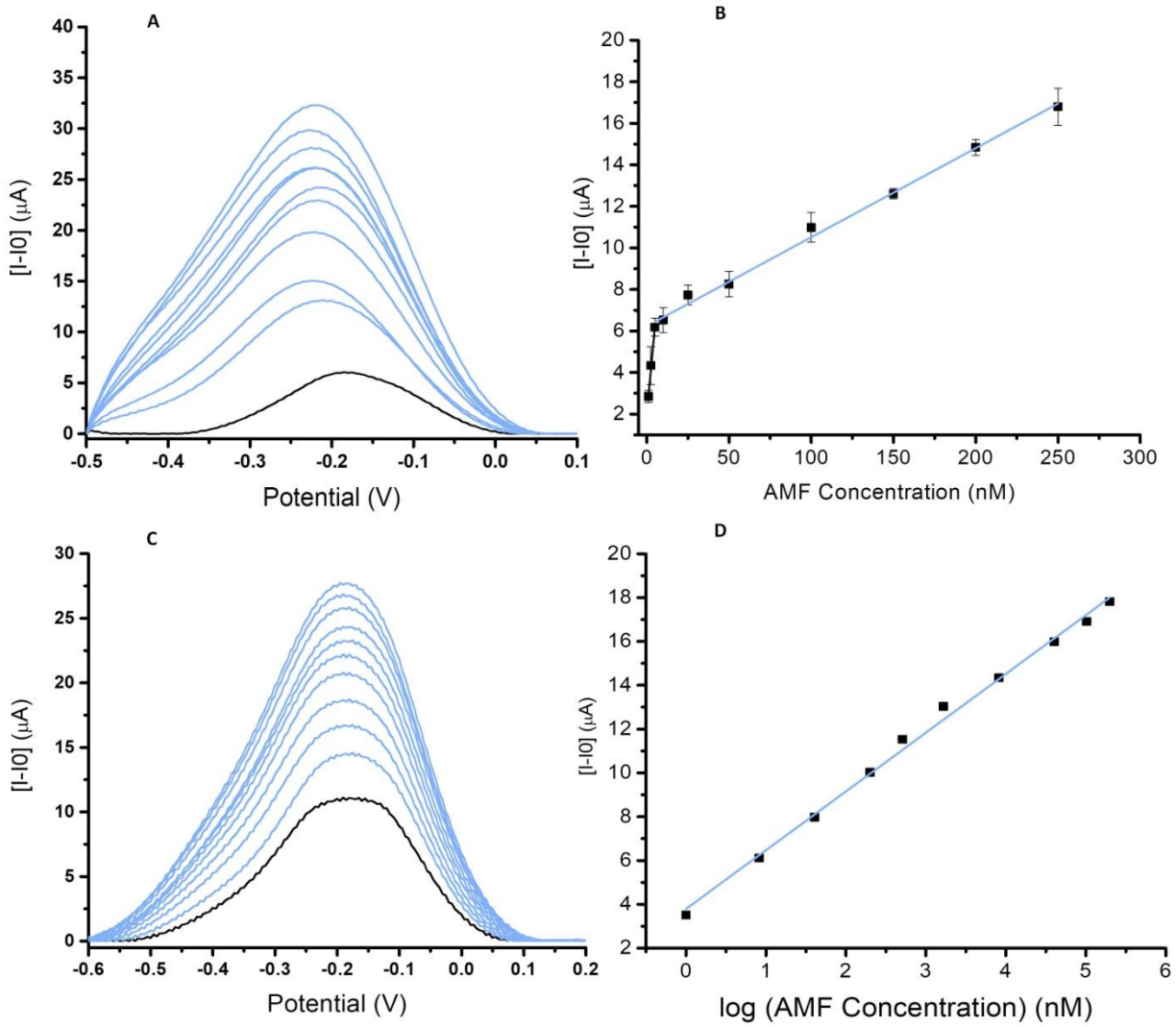

Figure 3. (A) DPVs response registered for nanoMIPs to AMF solutions of different concentrations from 1 nM to 250 nM in PBS after 30 minutes incubation. (**B)** Calibration curves obtained for the same concentrations of AMF (two different linear correlations between the increase of the current intensity and the concentration of AMF were found). **(C)** DPVs response registered for nanoMIPs composite (GPHOx and chitosan) to AMF solutions of different concentrations from 1 nM to 200 nM in PBS after 30 minutes incubation. (**D)** Calibration curve obtained for the same concentrations of AMF. Black curves represents the voltammograms obtained in PBS in the absence of AMF (I0).

In **Figure 4** the differences between the current intensities obtained after the incubation with different concentrations of AMF and the current obtained after 30 minutes of contact with 0.1 M PBS of pH 7.4 (no AMF in this solution) were compared. The equations of the corresponding calibration curves and the analytical parameters relevant for comparison are presented in **Table S4 (*Supplementary information S2 2.5*).** This table presents, the comparison between the analytical parameters obtained after the preconcentration of AMF on the SPEs modified with

nanoMIPs and chitosan, and nanoMIPs, chitosan and reduced GPHOx (rGPHOx), respectively, after the incubation on the chitosan-based optimized platform and on the bare electrode. From **Figure 4** it can be observed that the ferrocene signal is proportional with the concentration of the incubated AMF solution only on the electrodes modified with nanoMIPs: Chitosan 2:1 (c – green) and with nanoMIPs: Chitosan 2:1+ rGPHOx (d – blue), so it can be concluded that the nanoMIPs facilitate the AMF immobilization at the nanoMIPs-based sensors and its indirect detection via the ferrocene electrochemical oxidation. It can be observed in **Figure 4** and **Table S4** that the presence of nanoMIPs and rGPHOx causes a 10,000-fold increase in sensitivity, simultaneously with a decrease in LOQ and implicitly in LOD, which confirms the importance of using nanomaterials, namely rGPHOx for the functionalization of electrodes. The obtained results were compared with the results found in the literature and presented in **Table 1.** The trend of variation of the current signal with the concentration of AMF, observed in the case of the platform with nanoMIPs and GPHOx, is saturation, a phenomenon that is observed even at lower concentrations (curve d).

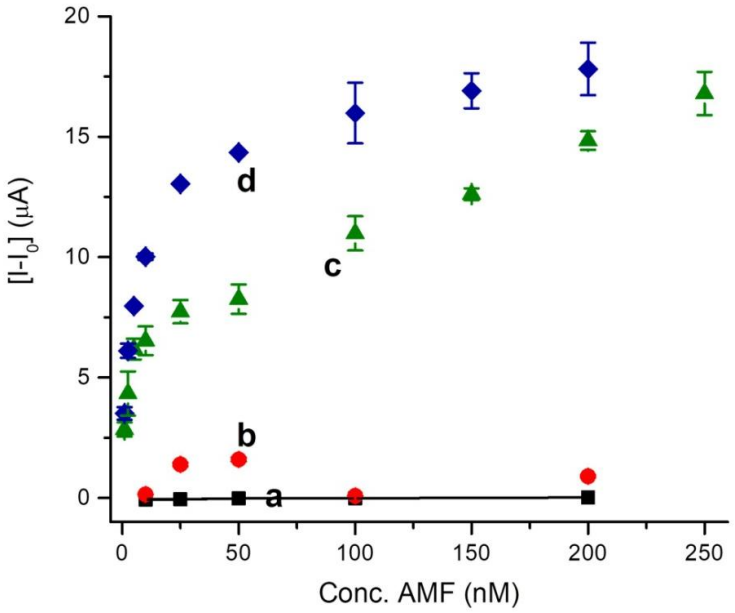

Figure 4. Calibration curves obtained for the same concentrations of AMF after the preconcentration on the (a - **black**■) bare graphite SPEs, (b - **red**●) SPEs modified with 2% chitosan (10 µL), (c - **green**▲) SPEs modified with nanoMIPs: Chitosan 2:1, and (d - **blue**♦) SPEs modified with nanoMIPs: Chitosan+rGPHOx = 2:1.

This phenomenon is not as accentuated in the case of the platform without GPHOx, where a linear dependence of the current is observed throughout the tested concentration range. Analytical performances were very close on both platforms, thus, it was decided that all subsequent tests should be performed on both types of sensors.

The analytical performance of the sensors based on nanoMIPs developed in the current study is comparable, or better than other sensors for AMF recently published and selected from the literature (see **Table 1**).

Sensors that have better analytical performance are generally suitable for the detection of AMF from biological samples [35,36], while the sensor reported in this manuscript can be easily adapted either for testing illicit street samples, or for laboratory tests, from biological samples collected from patients.

Taking into account that AMF does not have an electrochemical signal, direct electrochemical detection is not possible, so in some studies a derivatization step is mandatory [4,35]. The step that involves laborious detection protocols [36–38], which does not lend itself to rapid testing. For immunosensor-type systems, the use of antibodies poses problems of stability over time [39], and in the case of aptasensors, the immobilization of the aptamer on the surface of the transducer must be done in a carefully controlled manner to ensure reproducibility [40]. The relatively simple and fast immobilization method used in the current study proved viable and allowed obtaining nanocomposite surfaces with good stability, and the presence of nanoMIPs and graphenes additionally ensures good selectivity and sensitivity for the target.

Table 1. Electrochemical sensors for AMP detection – comparison of optimized sensor performance with literature data

Technique	**Type of electrode (E)**	**LOD (nM)**	**Linear range (nM)**	**Real samples/ Recovery (%)**	**Ref**
A	Ab/PtE	$2.5*10^3$	$740 – 14.8*10^3$	-	[39]
ECL	$Ru(bpy)_3]^{2+}$ – Nafion composite/GCE	0.05	$5*10^3 – 10*10^5$	-	[36]
A/ transistor	Cucurbit[7]uril/gold E	$1*10^{-3}$	0.001 - 1000	-	[37]
CV SWV	Gold E	$30.9*10^3$	$110.9*10^3$ - $258.9*10^3$	Urine/ 97.4 – 98.5	[41]
PT	ISE	$12*10^3$	$1*10^4$ - $1*10^6$		[38]
SWV	SPEs	$22.2*10^3$	$5*10^4$ - $50*10^4$	Drug seizures/ 83 – 113.6	[4]

SWV	PFA-coated SPEs	$3*10^5$	$5*10^5 – 1.25*10^6$	-	[35]
DPV	Apt/AuNF/Au	0.51	0.1 – 1	Urine/ 99 – 104 Water 94.3–105	[40]
DPV	**nanoMIPs/chitosan-based SPEs**	**0.3**	**1 – 250**	Drug seizures/ **96.8-111.7**	**This work**
DPV	**nanoMIPs/chitosan/ GPHOx-based SPEs**	**0.3**	**1 – 200**	Drug seizures/ **100.9-107.6**	**This work**

Abbreviations: Ab: Antibody; A: amperometry; ECL: Electrochemiluminiscence; GCE: glassy carbon electrode; LOD : Limit of detection; PtE: platinum electrode; SWV: square-wave voltammetry; SPEs: Graphite screen-printed electrodes; PFA: Paraformaledehyde; Apt: Aptamer, AuNF: gold nanoflowers; DPV: Differential pulse voltammetry; PT: Potentiometry; ISE: Ion-selective electrode, nanoMIPs: Nano molecular imprinted polymers; GPHOx: Graphene oxide.

3.4. Selectivity and stability of the sensors

Three solutions containing 100 nM AMF + 100 nM MDMA, 100 nM AMF + 100 nM cocaine, and 100 nM AMF + 100 nM methamphetamine, respectively were incubated on graphite SPEs modified with chitosan 0.5 mg mL^{-1} and an ethanolic suspension of nanoMIPs 0.1 mg mL^{-1} (**Figure 5(A)**), and on the graphite SPEs modified with chitosan 0.5 mg mL^{-1} and rGPHOx 1 mg mL^{-1}**,** and an ethanolic solution of nanoMIPs 0.1 mg mL^{-1} (**Figure 5(B)**) for 30 minutes.

In the case of the sensors modified only with nanoMIPs and chitosan the DPVs are presented for the equimolar concentrations of AMF and cocaine, the obtained DPV is compared with the DPV of 100 nM AMF. An average recovery of 106.4% was obtained for the target drug of abuse in the presence of equal concentration of cocaine.

In the case of the equimolar concentrations of AMF and MDMA, an average recovery of 101.99% proves that AMF can be detected if combined in a 1: 1 combination ratio with MDMA. It can be also observed in **Figure 5(A)** that a 1:1 combination ratio between AMF and methamphetamine does not hinder the detection of the target, since a recovery of 98.28% was obtained for AMF oxidation signal registered with the optimized electrochemical sensor functionalized with nanoMIPs.

In the case of the electrochemical sensor containing GPHOx in the composite film (**Figure 5 (B)**) an average recovery of 100.65% was obtained for the target analyte in the presence of equal concentration of MDMA, 100.17% in the presence of equal concentration of cocaine, and 96.94% in the presence of equal concentration of methamphetamine.

All results obtained from the selectivity study, on both optimized platforms are centralized in **Table S5 (*Supplementary information S2 2.6*)**.

.

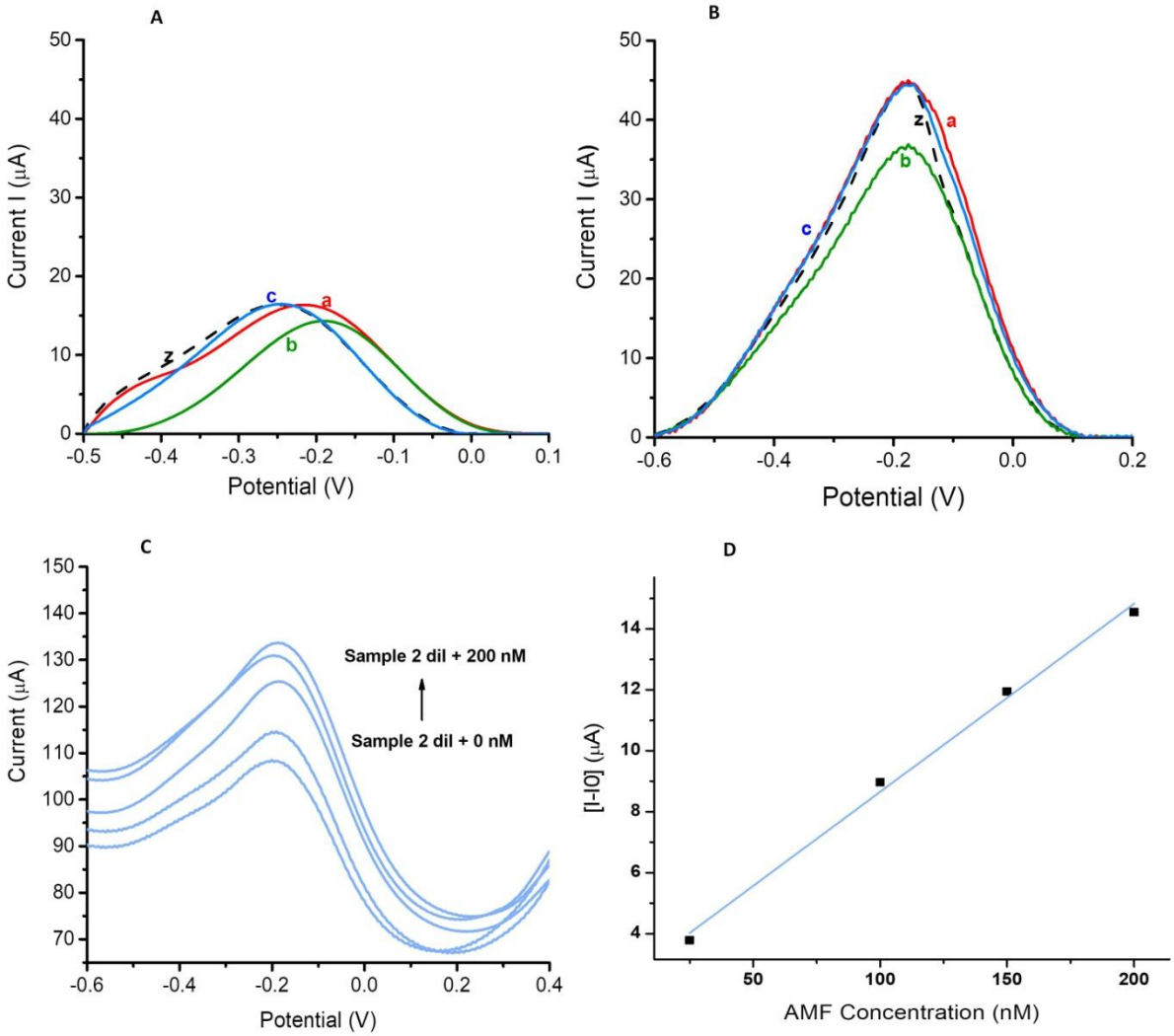

Figure 5. Comparison between the signal obtained using the sensor based on nanoMIPs and chitosan **(A), or** obtained using the sensor based on nanoMIPs, chitosan and rGPHOx (**B**) after the preconcentration fron different solutions containing 100 nM AMF (**z - black**) and 100 nM AMF + 100 nM MDMA (**a - red**), 100 nM AMF + 100 nM methamphetamine (**b - green**), and 100 nM AMF + 100 nM cocaine (**c - blue**), obtained using the sensor based on nanoMIPs, chitosan and rGPHOx. DPVs obtained with the optimized sensor based on graphite SPEs functionalized with chitosan, rGPHOx and nanoMIPs composite film **(C)** after the preconcentration with solution containing equal volumes of Sample 2 and standard solutions of AMF of known concentrations. The calibration curve for Sample 2 using the standard addition method on graphite SPEs functionalized with chitosan, rGPHOx and nanoMIPs/ composite film **(D)**. The concentration of standard tested were: 25 nM; 50 nM; 100 nM; 150 nM; 200 nM and 250 nM. The street sample was first dissolved in MeOH and diluted 50 000 times before use for DPV tests.

3.5. Real samples analysis - seized illicit drug samples assessment

Two street seized samples were analyzed by DPV using the optimized sensors. Increasing concentrations of AMF were incubated on the graphite SPEs modified with chitosan 0.5 mg mL^{-1}, rGPHOx 1 mg mL^{-1} and nanoMIPs suspension 0.1 mg mL^{-1} in a combination ratio of 1:2. After 30 minutes of incubation, each electrode was washed with 1 mL of 0.1 M PBS of pH 7.4. DPV tests were performed using 100 µL of the same buffer solution. The amount of AMF contained in each sample was determined using the standard addition method by using AMF standard solutions of known concentration. The initial solution containing unknown amount of illicit drug was diluted 150 000 times for the first sample containing AMF (denoted here as Sample 1). The difference between current intensities obtained at different concentrations and the current intensity obtained after the incubation with a buffer solution containing 0 nM AMF were computed, and a concentration of 1390.84 µg mL^{-1} was calculated for AMF in the case of real Sample 1 by using the chitosan, GPHOx and nanoMIPs composite based sensor (**Table S6 (*Supplementary information S2 2.7)*)**. The same experimental procedure was applied for Sample 2 except the dilution which has been in this case only 50 000 times. The obtained DPVs are presented in **Figure 5(C).** In the calibration curve represented in **Figure 5(D)**, the difference between current intensities obtained at different concentrations and the current intensity obtained after the incubation with a buffer solution containing 0 nM AMF were represented. A concentration of 543.53 µg mL^{-1} was calculated for AMF in the case of real Sample 2 by using the chitosan, rGPHOx and nanoMIPs composite based sensor **(Table S6 (*Supplementary information S2 2.7*)).**

The real street samples named Sample 1 and Sample 2 were tested using an optimized UPLC-MS procedure. The analytical results are presented compared to those obtained with the sensor based on SPEs of graphite modified with chitosan and nanoMIPs composite film and chitosan, rGPHOx and nanoMIPs film in **Table S6 (*Supplementary information S2 2.7*)**.

The recoveries obtained with the optimized sensor modified with nanoMIPs with chitosan and rGPHOx in a combination ratio of 2:1 are higher than those obtained for the optimized sensor modified only with nanoMIPs and chitosan. This proves the electrocatalytic effect of rGPHOx, which causes an increase in the electrochemically active surface, and after the electrochemical reduction, causes an increase in the number of sites where nanoMIPs are immobilized, and implicitly in an increase in the sensitivity of the sensor for AMF detection.

4. Conclusions

Electrochemical molecularly imprinted nanopolymer particles were synthesized for the selective detection of AMF based on the ferrocene signal as a redox probe embedded in the nanopolymer matrix. An innovative immobilization method was applied for the first time consisting in the use of chitosan, as such or in combination with rGPHOx to improve the electrochemically active surface and the conductive properties of the functionalized surface of the sensor. It was demonstrated that the ferrocenyl group acted as the redox probe, sensitive and highly selective to

the presence of AMF molecules in the imprinted cavities. The binding of AMF was indeed detected by an increase of the current intensity of the ferrocene oxidation. A linear variation of the difference of current intensity upon the AMF concentration was measured on several sensors, thus proving the reliability of the sensor. A LOD of 0.3 nM was obtained, as well as high selectivity towards cocaine, MDMA and methamphetamine. The optimized sensor platform seemed to be very promising and easy to adapt for the electrochemical detection of other compounds with practical importance such as biomarkers, drugs, or pollutants.

5. Funding

This project has received funding from the European Union's Horizon 2020 Research and Innovation Programme under grant agreement no. 833787, and from the research project no. PCD 774/5/11.01.2023, grated by "Iuliu Haţieganu" University of Medicine and Pharmacy Cluj-Napoca.

Bibliography

[1. Florea, A.; de Jong, M.; De Wael, K. Electrochemical strategies for the detection of forensic drugs. *Curr. Opin. Electrochem.* **2018**, *11*, 34–40, doi:10.1016/j.coelec.2018.06.014.

2. Berman, S.M.; Kuczenski, R.; McCracken, J.T.; London, E.D. Potential adverse effects of amphetamine treatment on brain and behavior: A review. *Mol. Psychiatry* **2009**, *14*, 123–142, doi:10.1038/mp.2008.90.

3. Bramness, J.G.; Gundersen, Ø.H.; Guterstam, J.; Rognli, E.B.; Konstenius, M.; Løberg, E.M.; Medhus, S.; Tanum, L.; Franck, J. Amphetamine-induced psychosis - a separate diagnostic entity or primary psychosis triggered in the vulnerable? *BMC Psychiatry* **2012**, *12*, doi:10.1186/1471-244X-12-221.

4. Parrilla, M.; Felipe Montiel, N.; Van Durme, F.; De Wael, K. Derivatization of amphetamine to allow its electrochemical detection in illicit drug seizures. *Sensors Actuators, B Chem.* **2021**, *337*, 129819, doi:10.1016/j.snb.2021.129819.

5. Carvalho, M.; Carmo, H.; Costa, V.M.; Capela, J.P.; Pontes, H.; Remião, F.; Carvalho, F.; De Lourdes Bastos, M. Toxicity of amphetamines: An update. *Arch. Toxicol.* **2012**, *86*, 1167–1231, doi:10.1007/s00204-012-0815-5.

6. Robinson, T.E.; Berridge, K.C. The psychology and neurobiology of addiction: an incentive-sensitization view. *Addiction* **2000**, *95 Suppl 2*, doi:10.1080/09652140050111681.

7. European drug report 2020 - Publications Office of the EU.

8. EU drug markets report 2019 - Publications Office of the EU.

9. EMCDDA.

10. Cuypers, E.; Bonneure, A.J.; Tytgat, J. The use of presumptive color tests for new psychoactive substances. *Drug Test. Anal.* **2016**, *8*, 137–141, doi:10.1002/dta.1847.

11. Dragan, A.M.; Parrilla, M.; Feier, B.; Oprean, R.; Cristea, C.; De Wael, K. Analytical techniques for the detection of amphetamine-type substances in different matrices: A comprehensive review. *TrAC Trends Anal. Chem.* **2021**, *145*, 116447, doi:10.1016/J.TRAC.2021.116447.

12. Płotka, J.M.; Biziuk, M.; Morrison, C. Common methods for the chiral determination of amphetamine and related compounds I. Gas, liquid and thin-layer chromatography. *TrAC - Trends Anal. Chem.* **2011**, *30*, 1139–1158, doi:10.1016/j.trac.2011.03.013.

13. Gerace, E.; Seganti, F.; Luciano, C.; Lombardo, T.; Di Corcia, D.; Teifel, H.; Vincenti, M.; Salomone, A. On-site identification of psychoactive drugs by portable Raman spectroscopy during drug-checking service in electronic music events. *Drug Alcohol Rev.* **2019**, *38*, 50–56, doi:10.1111/dar.12887.

14. Alanazi, K.; Garcia Cruz, A.; Di Masi, S.; Voorhaar, A.; Ahmad, O.S.; Cowen, T.; Piletska, E.; Langford, N.; Coats, T.J.; Sims, M.R.; et al. Disposable paracetamol sensor based on electroactive molecularly imprinted polymer nanoparticles for plasma monitoring. *Sensors Actuators, B Chem.* **2021**, *329*, 129128, doi:10.1016/j.snb.2020.129128.

15. Graham, S.P.; El-Sharif, H.F.; Hussain, S.; Fruengel, R.; McLean, R.K.; Hawes, P.C.; Sullivan, M. V.; Reddy, S.M. Evaluation of Molecularly Imprinted Polymers as Synthetic Virus Neutralizing Antibody Mimics. *Front. Bioeng. Biotechnol.* **2019**, *7*, 1–7, doi:10.3389/fbioe.2019.00115.

16. Azevedo, M.; Luiz, J.; Cardoso, A.; Sá, D.; Buffon, E. Electrochemical sensors based on molecularly imprinted polymer on nanostructured carbon materials : A review. *J. Electroanal. Chem.* **2019**, *840*, 343–366, doi:10.1016/j.jelechem.2019.04.005.

17. Mazzotta, E.; Turco, A.; Chianella, I.; Guerreiro, A.; Piletsky, S.A.; Malitesta, C. Solid-phase synthesis of electroactive nanoparticles of molecularly imprinted polymers. A novel platform for indirect electrochemical sensing applications. *Sensors Actuators, B Chem.* **2016**, *229*, 174–180, doi:10.1016/j.snb.2016.01.126.

18. Canfarotta, F.; Poma, A.; Guerreiro, A.; Piletsky, S. Solid-phase synthesis of molecularly imprinted nanoparticles. *Nat. Protoc.* **2016**, *11*, 443–455, doi:10.1038/nprot.2016.030.

19. Garcia-Cruz, A.; Ahmad, O.S.; Alanazi, K.; Piletska, E.; Piletsky, S.A. Generic sensor platform based on electro-responsive molecularly imprinted polymer nanoparticles (e-NanoMIPs). *Microsystems Nanoeng.* **2020**, *6*, doi:10.1038/s41378-020-00193-3.

20. Paul, F.; Weikl, T.R. How to Distinguish Conformational Selection and Induced Fit Based on Chemical Relaxation Rates. *PLoS Comput. Biol.* **2016**, *12*, 1–17, doi:10.1371/journal.pcbi.1005067.

21. Vogt, A.D.; Di Cera, E. Conformational selection or induced fit? A critical appraisal of the kinetic mechanism. *Biochemistry* **2012**, *51*, 5894–5902, doi:10.1021/BI3006913.

22. Udomsap, D.; Branger, C.; Culioli, G.; Dollet, P.; Brisset, H. A versatile electrochemical sensing receptor based on a molecularly imprinted polymer. *Chem. Commun.* **2014**, *50*, 7488–7491, doi:10.1039/C4CC02658F.

23. Ekomo, V.M.; Branger, C.; Bikanga, R.; Florea, A.M.; Istamboulie, G.; Calas-Blanchard, C.; Noguer, T.; Sarbu, A.; Brisset, H. Detection of Bisphenol A in aqueous medium by screen printed carbon electrodes incorporating electrochemical molecularly imprinted polymers. *Biosens. Bioelectron.* **2018**, *112*, 156–161, doi:10.1016/J.BIOS.2018.04.022.

24. Garcia-Cruz, A.; Cowen, T.; Voorhaar, A.; Piletska, E.; Piletsky, S.A. Molecularly imprinted nanoparticles-based assay (MINA) – detection of leukotrienes and insulin. *Analyst* **2020**, *145*, 4224–4232, doi:10.1039/D0AN00419G.

25. Cowen, T.; Karim, K.; Piletsky, S. Computational approaches in the design of synthetic receptors - A review. *Anal. Chim. Acta* **2016**, *936*, 62–74, doi:10.1016/J.ACA.2016.07.027.

26. Armbruster, D.A.; Pry, T. Limit of Blank, Limit of Detection and Limit of Quantitation. *Clin. Biochem. Rev.* **2008**, *29*, S49.

27. Ali, I.; Suhail, M.; Alothman, Z.A.; Abdulrahman, A.; Aboul-Enein, H.Y. Drug analyses in human plasma by chromatography. *Handb. Anal. Sep.* **2020**, *7*, 15–46, doi:10.1016/B978-0-444-64066-6.00002-2.

28. Ahuja, S. Overview: Handbook of pharmaceutical analysis by HPLC. *Sep. Sci. Technol.* **2005**, *6*, 1–17, doi:10.1016/S0149-6395(05)80045-5.

29. Danaei, M.; Dehghankhold, M.; Ataei, S.; Hasanzadeh Davarani, F.; Javanmard, R.; Dokhani, A.; Khorasani, S.; Mozafari, M.R. Impact of particle size and polydispersity index on the clinical applications of lipidic nanocarrier systems. *Pharmaceutics* **2018**, *10*, 1–17, doi:10.3390/pharmaceutics10020057.

30. Ehsani, A.; Bigdeloo, M.; Assefi, F.; Kiamehr, M.; Alizadeh, R. Ternary nanocomposite of conductive polymer/chitosan biopolymer/metal organic framework: Synthesis, characterization and electrochemical performance as effective electrode materials in pseudocapacitors. *Inorg. Chem. Commun.* **2020**, *115*, 107885, doi:10.1016/J.INOCHE.2020.107885.

31. Adumitrăchioaie, A.; Tertiș, M.; Suciu, M.; Graur, F.; Cristea, C. A novel immunosensing platform for serotonin detection in complex real samples based on graphene oxide and chitosan. *Electrochim. Acta* **2019**, *311*, 50–61, doi:10.1016/j.electacta.2019.04.128.

32. Tertis, M.; Sîrbu, P.L.; Suciu, M.; Bogdan, D.; Pana, O.; Cristea, C.; Simon, I. An Innovative Sensor Based on Chitosan and Graphene Oxide for Selective and Highly-Sensitive Detection of Serotonin. *ChemElectroChem* **2022**, *9*, e202101328, doi:10.1002/CELC.202101328.

33. Huang, J.; Qiu, Z.; Lin, J.; Lin, J.; Zhu, F.; Lai, G.; Li, Y. Ultrasensitive determination of metronidazole using flower-like cobalt anchored on reduced graphene oxide nanocomposite electrochemical sensor. *Microchem. J.* **2023**, *188*, 108444, doi:10.1016/J.MICROC.2023.108444.

34. Huang, H.; Xia, Y.; Tao, X.; Du, J.; Fang, J.; Gan, Y.; Zhang, W. Highly efficient electrolytic exfoliation of graphite into graphene sheets based on Li ions intercalation–expansion–microexplosion mechanism. *J. Mater. Chem.* **2012**, *22*, 10452–10456, doi:10.1039/C2JM00092J.

35. Schram, J.; Parrilla, M.; Slosse, A.; Van Durme, F.; Åberg, J.; Björk, K.; Bijvoets, S.M.; Sap, S.; Heerschop, M.W.J.; De Wael, K. Paraformaldehyde-coated electrochemical sensor for improved on-site detection of amphetamine in street samples. *Microchem. J.* **2022**, *179*, doi:10.1016/j.microc.2022.107518.

36. McGeehan, J.; Dennany, L. Electrochemiluminescent detection of methamphetamine and amphetamine. *Forensic Sci. Int.* **2016**, *264*, 1–6, doi:10.1016/j.forsciint.2016.02.048.

37. Jang, Y.; Jang, M.; Kim, H.; Lee, S.J.; Jin, E.; Koo, J.Y.; Hwang, I.C.; Kim, Y.; Ko, Y.H.; Hwang, I.; et al. Point-of-Use Detection of Amphetamine-Type Stimulants with Host-Molecule-Functionalized Organic Transistors. *Chem* **2017**, *3*, 641–651, doi:10.1016/j.chempr.2017.08.015.

38. Gallardo-Gonzalez, J.; Saini, A.; Baraket, A.; Boudjaoui, S.; Alcácer, A.; Streklas, A.; Teixidor, F.; Zine, N.; Bausells, J.; Errachid, A. A highly selective potentiometric amphetamine microsensor based on all-solid-state membrane using a new ion-pair complex, [3,3″-Co(1,2-closo-C2B9H11)2]− [C9H13NH]+. *Sensors Actuators, B Chem.* **2018**, *266*, 823–829, doi:10.1016/j.snb.2018.04.001.

39. Ivison, F.M.; Kane, J.W.; Pearson, J.E.; Kenny, J.; Vadgama, P. Development of a redox mediated amperometric detection system for immunoassay. Application to urinary amphetamine screening. *Electroanalysis* **2000**, *12*, 778–785, doi:10.1002/1521-4109(200006)12:10<778::AID-ELAN778>3.0.CO;2-#.

40. Soni, S.; Jain, U.; Burke, D.H.; Chauhan, N. A label free, signal off electrochemical aptasensor for amphetamine detection. *Surfaces and Interfaces* **2022**, *31*, 102023, doi:10.1016/j.surfin.2022.102023.

41. Nevešcanin, M.M.; Avramov Ivic, M.L.; Petrovic, S.D.; Mijin, D.Ž.; Banovic Stevic, S.N.; Jovanovic, V.M. The use of a gold electrode for the determination of amphetamine derivatives and application to their analysis in human urine. *J. Serbian Chem. Soc.* **2013**, *78*, 1373–1385, doi:10.2298/JSC121228032N.